INTERACTION OF A HOLLOW CATHODE STREAM WITH A HALL THRUSTER

L. Albarède, V. Lago, P. Lasgorceix, M. Dudeck
Laboratoire d'Aérothermique, 1C avenue de la Recherche Scientifique, 45071 Orléans cedex, France
A.I. Bugrova
Moscow State Institute of Radio-Engineering Electronics and Automation, MIREA, Laboratory of Plasmotics, 78, 117454, Moscow, Russia
K. Malik
Imperial College, London, Great-Britain

Abstract :

The hollow cathode is one of the main sub-element of the design of Hall thrusters for satellites. The flow of the electrons emitted by the cathode is used in one hand to supply the discharge in the channel of the thruster and in the other hand to electrically neutralize the plasma plume. The study of the different phenomena appearing in a hollow cathode and in the plasma plume near the hole of the cathode present a great interest for the knowledge of its interactions[6-16] with the behaviour of the thruster. The properties of the electrons incoming in the channel are depending on the prevalent magnetic and electrostatic potential maps. In particular, it is important to examine the electron flux and to determine which are the interactions between its characteristics (density, electron temperature, energy distribution, fluctuations) and the properties of the main discharge.

A study of three different cathodes has been carried out in the French PIVOINE test facility, two called 'cold cathodes' and one called 'hot cathode'. Hot cathodes need a heating power source while the electron emission is sustained by the plasma for the cold cathodes. The tests have been performed with the Hall thruster SPT100-ML (laboratory model, nominal conditions: 300V, 5mg/s) under identical operating conditions and using the same sensors. In order to compare the interaction of these cathodes with the thruster behaviour, we have measured systematically the axial thrust, the discharge current (mean value and transient evolution), the ionic current in the plume, and the cathode potential. In addition, optical and electrostatic probe measurements have been used to characterize the plasma near the cathode orifice. These diagnostics gave information on electron properties (density, energy distribution function, electron temperature) and emission of Xe* and Xe^{+}*. A CCD camera has been used to observe the plasma emission with interferential filters in the zone between the cathode and the exit of the thruster

This study aims to determine the boundary conditions of the discharge at the cathode, to control these conditions, leading to the optimisation of the performances of the Hall thrusters.

Introduction

The study of the cathodes has been performed in the PIVOINE test facility. Main technical characteristics are : 4m length, 2.2m diameter, 70000 l/s cryogenic pumping speed for xenon ensuring 2.5 10^{-5} mbar pressure for a xenon mass flow rate of 5 mg/s. Two lock chambers are used, one for the thruster and the other for the intrusive diagnostics. Permanently, the facility is equipped with a process control system and with a set of diagnostics (thrust balance, electric probes, ion energy analyser RPA, fast recording system). The thrusters (figure 1) currently used in PIVOINE is a SPT100 ML type with an hot hollow cathode (from MIREA, Moscow).
For the presented study, the tests have been performed with the usual MIREA cathode and with two cathodes: a hot hollow cathode developed by the KhAI institute (Ukraine), and a cold hollow cathode developed by LABEN Proel (Italy). We have taken care to keep the same position of the different cathodes relatively to the thruster channel (at 2.5 cm from the exhaust of the thruster and with angle of 50° with the thruster axis). The working points were chosen to have the most relevant comparisons.

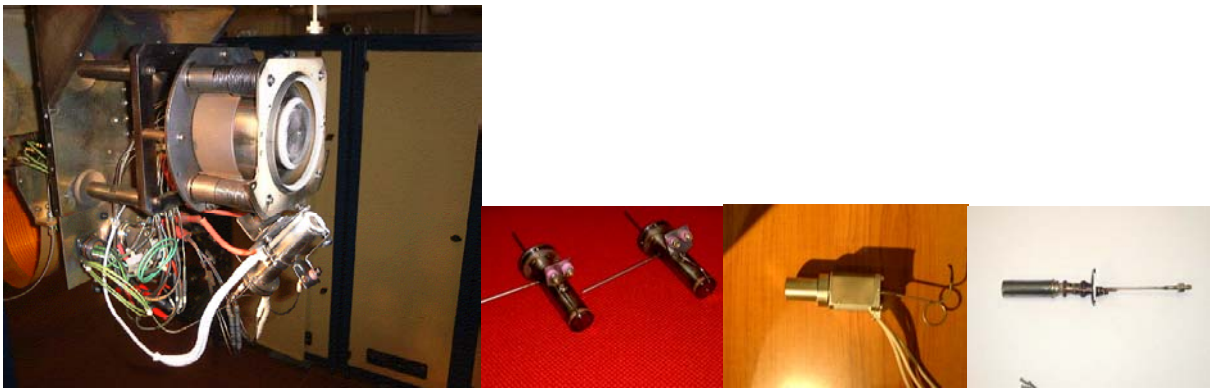

Figure 1: Photograph of the SPT100-ML in the PIVOINE facility with two electrostatic probes: beside the body of the cathode and close to the exit plane of the thruster (top).
Figure 2: The three tested hollow cathodes (MIREA, LABEN, KhAI)

Description of the cathodes

Since 1996, the usual cathode used in the facility test PIVOINE is a hot hollow cathode built by the MIREA (Russia). The pastille of this cathode is LaB_6 emitter heated by an electric current (about 13 A) crossing a rolled up tungsten wire. Heat screens and ceramic insulators allow a discharge current up to 6A. The size of the orifice is 3.5mm and the nominal cathode mass flow rate is 0.4mg/s.
The second one is a cold hollow cathode from LABEN Proel in Italy. It requires a step by step procedure of heater (0.5A to reach 8A). After the end of this procedure, it works without contribution of heating current. Its nominal flow rate is of 0.4 mg/s and its orifice is of 1mm diameter. This latter is made of porous tungsten, impregnated with products to reduce the work function. These products are brought by thermo-ionic emission temperature by means of a heated filament (Heater) wound around the cathode tube and insulated by a potting compound. An electrode (Keeper), biased positive with respect to the hollow cathode body, serve to accelerate the electrons. This way it assists in initiating and stabilising the electrical discharge. Once the discharge is ignited, the heater is switched-off and the plasma is maintained thanks to positive ion bombardment onto the insert surface. This cathode has been previously tested by SNECMA Moteurs on the PPS1350 with success.

The third hollow cathode comes from KhAI in Ukraine. This cathode has a ignition procedure which is a short impulse breakdown of 800V and needs a very low current applied on the wall of the cathode. This current plays the role of keeper at the start. Once this procedure is realized, the cathode works without outside contribution of energy. Its orifice is of 0.2; 0.4 mm and the nominal flow rate is 0.2 mg/s.

Macroscopic results

The study of the three hollow cathodes has been done by varying parameters like cathode and anode mass flow rates (m_a, m_c), voltage discharge (V_d) of SPT 100-ML and the heater current for the hot cathode (MIREA). The thrust has been measured. The discharge current (I_d) and the oscillations have been recorded with a fast recording acquisition system (for standard deviation, main frequency, Fourier transform etc…).
We evaluated the global efficiency η:

$$\eta = \frac{F^2}{2(U_d I_d + U_b I_b + U_c I_c)(m_c + m_a)}$$

where "d" means discharge, "b" means magnetic, "c" means cathode and "a" anode.

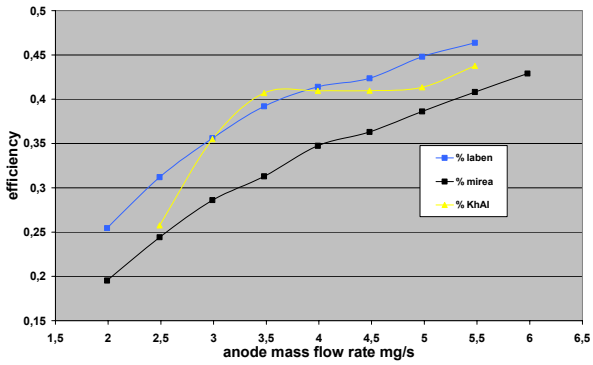

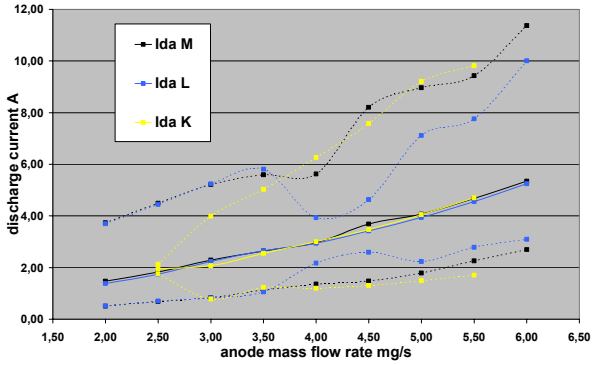

Figure 3: Efficiency as a function of anode mass flow rate (black: MIREA, yellow: KhAI, blue: LABEN)
Figure 4: discharge current as function of anode mass flow rate (black: MIREA, yellow: KhAI, blue: LABEN (full lines mean value, dotted lines min & max oscillations)

In figure 3 it can be observed that the efficiency generally increases with the anode mass flow rate The greater values for the LABEN compared with the MIREA cathode is due on the heater current power consumed (LABEN cathode is a cold cathode). The KhAI cathode has a different behaviour. The efficiency reach a maximum at 3.5 mg/s, and then decreases to join the behaviour of the others cathodes for m_a=5.5mg/s.

The mean discharge current (with minimum and maximum limits of observed oscillations) for each cathode are presented in figure 4. With the increase of the anode mass flow rate, the discharge current increases that means that the cathode has to supply more electrons into the channel and in the plume to neutralize the charge, therefore the cathode has to supply more electrons. The behaviour of the three cathodes is the same. Nevertheless, oscillations around the mean value of the discharge current vary with the used cathode. Each one has its own oscillation regime. The study of the discharge current as function of the cathode mass flow rate shows different maximum and minimum of oscillations for I_d, but the behaviour of the mean value is (quiet) almost the same with the different cathodes.

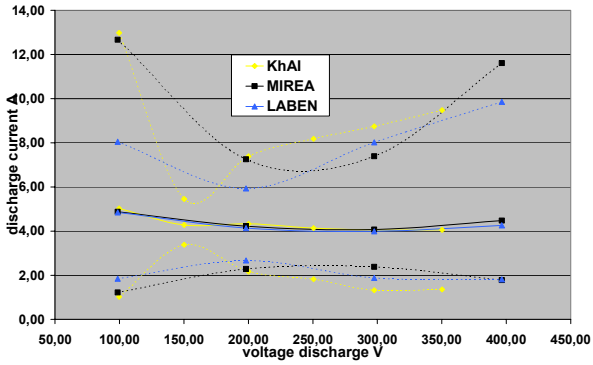

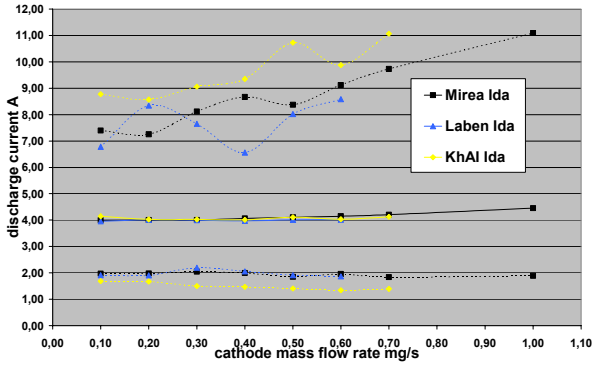

Figure 5: Discharge current as function of discharge voltage (black: MIREA, yellow: KhAI, blue: LABEN full lines mean value, dotted lines min & max oscillations)
Figure 6 : discharge current as function of cathode mass flow rate(full lines mean value, dotted lines max & min limits of observed oscillations)

The evolution of the spread of discharge current and its oscillations versus the voltage discharge is presented on the figure 5.
The three cathodes present a maximum of current oscillation before the value of 200V. This particular oscillation regime has been already observed with the MIREA cathode. In this special regime the oscillations are very high and the behaviour of the thruster is not stable. We call this zone the "partial ionisation" and "negative resistance" domain[3] before having the working fluctuation domain. Before reaching a normal regime oscillation, the oscillations of cathode present a minimum but not at the same value, MIREA at 250V, LABEN at 200V and KhAI at 150V. A stable region of functioning is then reached where the plasma discharge of the SPT is stable. Here, one can just observe that the cathode LABEN presents the lowest amplitude of oscillation among the three cathodes.

The figure 6 presents the variation of the discharge current with the cathode mass flow rate, we can note that the three cathodes have the same mean value of current but differ from their minimum and maximum of the current oscillation. It is interesting to note that the oscillations of the discharge currents are connected with the oscillations of the cathode potential, presented in the figure 7.

Especially, the variations of the maximum of the oscillation of the discharge current and the cathode potential are similar for the three cathodes.

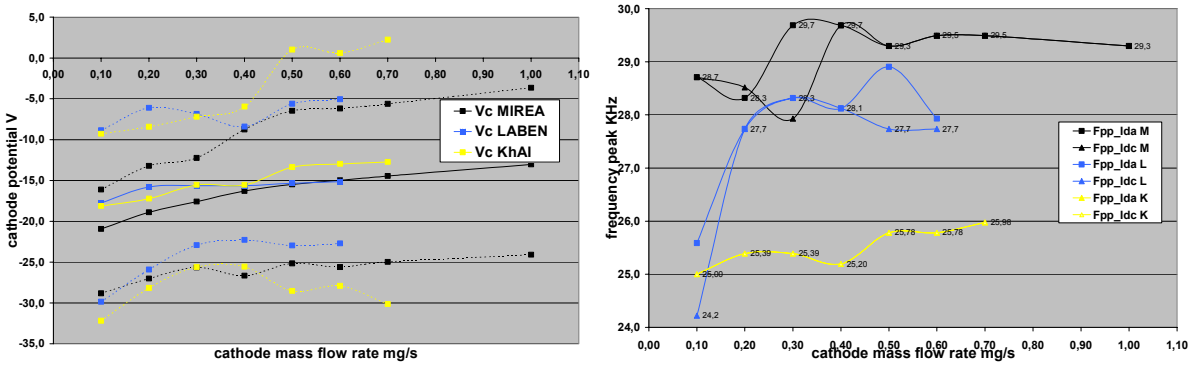

Figure 7: cathode potential as function of cathode mass flow rate(full lines mean value, dotted lines max & min of oscillations

Figure 8: frequency Main peak of discharge current (picked up on the anode line and on the cathode line) as function of cathode mass flow rate

The fall of cathode potential V_c, as the decreasing of cathode mass flow rate m_c, is connected to the main frequency peak of the Fourier transform of the discharge current (figure 8). This effect is appearing on the main peak of frequency discharge as function of the cathode mass flow rate: at each fall of V_c there's a fall of the frequency peak. This fall is recorded on the anode line of electric circuit like on the cathode line but not exactly on the same flow rate. An explanation of the link between the fall of cathode potential and frequency peak is that the discharge voltage is the difference of potential between the anode and the cathode $V_d=V_a-V_c$. In our case, the difference of potential between the anode and the cathode remained constant at $V_d=300V$, but the decrease of cathode mass flow rate implicates a potential fall that creates a fall of anode potential in the discharge ($V_a=V_d+V_c\approx 300-15=285V$). The main frequency peak can be connected to the oscillation of transit time of neutrals (as ions) in the discharge channel. A simple model[3] gives, within the present operating regime, a relation between frequency and voltage discharge.

$$f \approx \frac{1}{2\pi}\sqrt{V_i V_a} \approx \frac{1}{2\pi}\sqrt{V_a}\left(\frac{2e\Delta\phi}{M}\right)^{1/4}$$

where V_i is the velocity of ions, V_a the velocity of neutrals, $\Delta\phi$ difference of potential observed by the ion, and M the mass of ion. This formula indicates that within the present operating regime, the frequency of the oscillations is a function of the discharge voltage $\Delta\phi$ in the accelerating zone. This difference of potential depends on the cathode potential, which depends on the cathode mass flow rate as we have seen in fig 7. We touch here one of the limits of improvement of the performances of the thruster. If we want to increase the global efficiency, it is interesting to reduce the cathode flow but it acts on the fall of potential. Consequently, the ions are created in a zone where the difference of potential is less strong. That corresponds to a loss of velocity of ions and so to a less strong specific impulse of the thruster.

In conclusion of the presented comparison, we can indicate that the three hollow cathodes correctly answer at the request of the thruster. However, it seems that the cathode LABEN is well optimized for our SPT 100ML in the nominal point of functioning.

Cathode-discharge interactions

The role of the hollow cathode in SPT is to supply electrons in the channel in order to sustain the discharge and to neutralise the positive charges in the plume. The cathode zone can be considered as a secondary discharge which is a boundary condition of the main discharge. It as also a second source of neutrals which can influence the main discharge. The neutrals are ejected from the cathode with an angle of 40° towards the plume without dependence from potential and magnetic lines. A supplementary problem is that this outside and polarized external cathode modifies the electric potential map[5] and consequently modifies the main plasma discharge near the cathode. In a Hall thruster, all the elements of the discharge are axisymmetric (or quasi-axisymmetric) as magnetic field, neutral injection, and channel ceramic. However the cathode, due to its local outside situation, breaks the symmetry[13]. This breaking symmetry may have an effect on the discharge and this effect has been visualised with a CCD camera looking a profile plane at 90° of the exit of the thruster. By using interferential filters in front of the camera, we can observe a wavelength band which includes specific ionic lines or specific excited neutrals lines. The CCD measurements were done filtering the luminous intensity emitted in view to select the neutral emission and the ions emission.

The properties of the three filters are shown in the table 1. We cannot deduce an exact value of the intensity because of the wavelength band. However, the intensities are well correlated with the ions or neutrals behaviour. The recorded lines using the filter at 825nm are: 828nm (a resonant level) and line at 823.16nm (a metastable level). The optical moires on almost all the images are due to defaults of the intereferential filter. The figure 9 presents the energy transition schemes for the four Xenon observed lines.

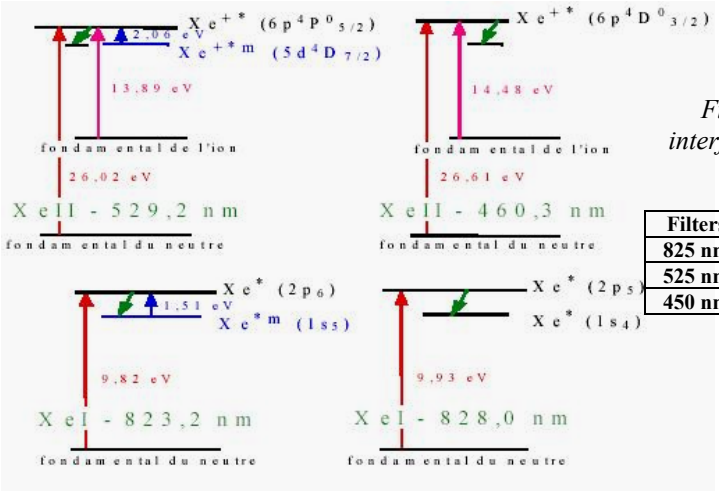

Figure 9: transition lines observed with the interferential filters, top ionic lines, down neutral lines[2].

Filters	Type	band	Lines 1	Lines 2	Lines 3
825 nm	Xe I	10 nm	823.16	828.01	834.68
525 nm	Xe II	8 nm	529.22	531.38	
450 nm	Xe II	15 nm	460.30	462.43	

Table 1: Description of filters[2]

The obtained images are matrices of size 512x512 pixels. The analysis of the images are done with the software MATLAB. Its allows to obtain a 3D map (r, z, intensity) normalized with regard to their acquisition time. The acquisition time are widely larger than those of the physical phenomena occurring in the channel. So, the images are not an instantaneous sight of the exit plan, but an average of the luminous intensity of this zone. An example is presented in the figure 10, where it can be distinguished the exit plane of the thrusters and the cathode luminous spot in the bottom of the image. This image was recorded with an interferential filter at 525 nm, and it presents the emission of Xenon ions at 529 nm. As it can be observed, the emission is more important on the channel exit in the opposite side of the cathode than on the nearest zone. This result is showed on the figure 11 with the intensity value versus the vertical axis of the thruster. The asymmetry with respect to the centre of the thrusters (at 325 pixels) is clearly visible.

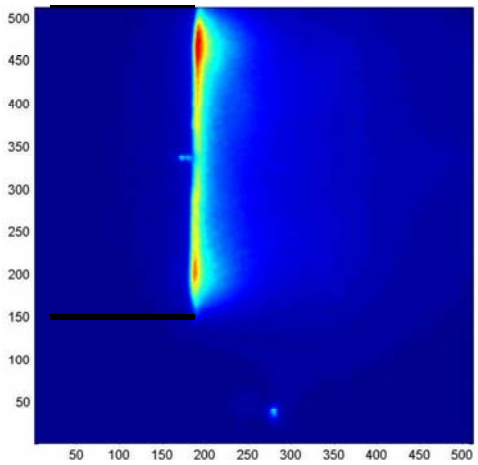

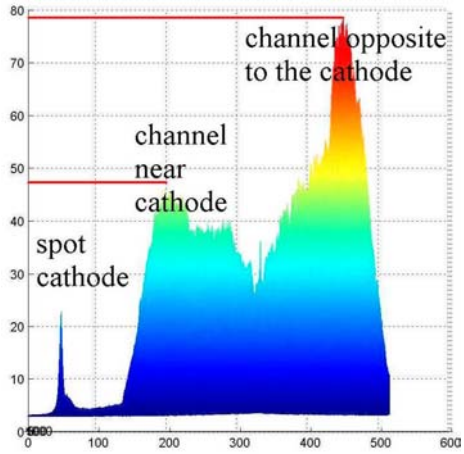

Figure 10: Image taken by CCD camera with filter 525 nm(ions)
Figure 11: Example of image with the filter at 525nm (ions) taken during the cathode LABEN experiment, treated by MATLAB to observe the asymmetry in the exit plan of the channel.

In view to quantify the asymmetry for the ions emission as well that for neutrals, we calculated the ratio of the maximum of intensity of the opposite side of the cathode (CE) over the near side of the cathode (CC). For each hollow cathode we calculated the ratio x = CE/CC as function of anode and cathode mass flow rate and discharge voltage (figure 12 and 13).

The value of x=CE/CC, is estimated with an error of 10%. As the voltage discharge, the dissymmetry increases for ions and neutrals lines. Measurements using both the filters 525nm and 450nm seem to give the same effect of dissymmetry for the ionic lines. This result agrees with optical spectroscopic measurements[4] showing that ions (450nm) are present in the exit plan and have a strong decrease towards the plume whereas, and that ions (525nm) are present in the exit plan with a smoother decrease in the plume. Therefore in the exit plan the two ionic lines should have the same behaviour.
The measurements done with the KhAI cathode presents the lowest dissymmetry for ions but the highest for neutrals. For neutrals x<1 with the cathode KhAI and x>1 with the others cathodes.
Figure 12, presents the x value for the ionic lines and shows that ions intensity is more intense in the channel opposite side to the cathode for the three cathodes. The cathode KhAI presents the lowest effect of the dissymmetry on ions intensity. One can remember that the cathode potential as function of cathode mass flow rate is the lowest for the KhAI cathode and the dimensions of the cathode body are small compare to the others.

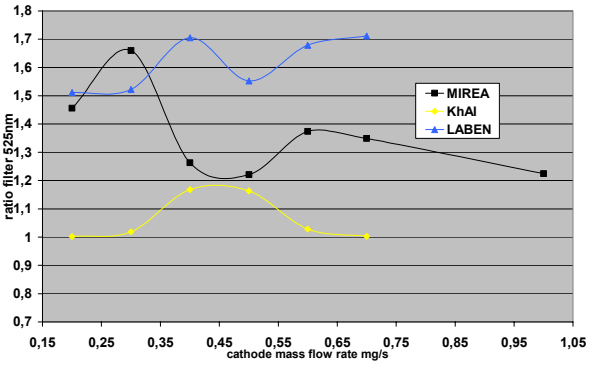

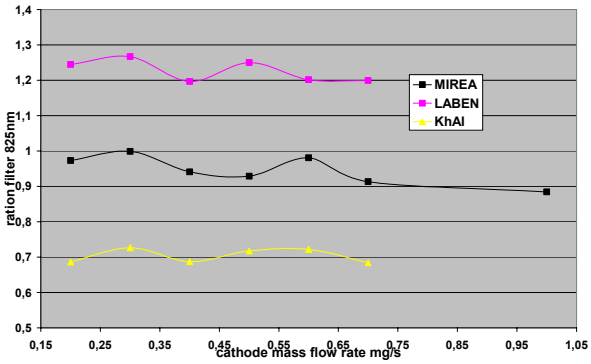

Figure 12 :Ratio CE/CC asymmetry 3 cathodes as function of cathode mass flow rate filter 525nm (ions)
Figure 13 : Ratio CE/CC asymmetry 3 cathodes as function of cathode mass flow rate filter 825nm (neutrals)

Figure 13 shows the ratio x of neutral lines with the filter 825nm as function of cathode mass flow rate. Following the uncertainties on x, the MIREA cathode seems to not have an effect on the symmetry but the two other cathodes present opposite dissymmetry for neutrals. The LABEN cathode has more neutral intensity on the opposite side of the cathode (CE) while the KhAI cathode has more neutral on the side near the cathode (CC). This effect of intensity of excited neutrals can be correlated with the energy and transport process of electrons. The neutrals are ejected from the cathode with a

thermal velocity not exactly in parallel of the exit plan but more in the direction of the plume (angle 40°). For Xenon neutral lines (figure 13), MIREA cathode has x<1 and LABEN x>1. This result is difficult to explain, we suppose that the dissymmetry is always in the same way for neutrals and ions but it seems that the design and the volume of the cathode can play a role. Ions are more intense at the opposite side of the cathode but neutrals intensity depends on the cathode type.

Figure 14 presents two views at the exit of the channel showing that the ceramic presents a non symmetric erosion. The side near the cathode presents more deeper faults than the side opposite to the cathode.

Figure 14 : left: ceramic of the thruster (channel side near the cathode)
right: ceramic of the thruster (channel side opposite to the cathode - 1400 hours of test)

These faults come from the ejection of ions having a very high velocity. These ions strike the ceramic because of the presence of a radial component of velocity v_r. It seems that this component is more important for the side near the cathode than on the opposite side. The v_r component could have as origin the deformation of equipotential[19] lines by the presence of the body of the cathode having an negative electric potential. An another possibility could be a default of alignment[7] between the ceramic and the thrusters axis. Therefore the ceramic would have her own axis which would be slightly different from the thrusters axis. The ceramic is perhaps not well perpendicular to the magnetic lines[7] in the acceleration area and produces a deviation of the ions by the magnetic lens toward the walls. Ions in the side near the cathode would be more divergent and do more collisions with the walls. The explanation by the electric potential of the cathode has our favour because this asymmetry on the erosion of ceramic has been observed in other laboratories. In any case, all these asymmetric problems seem to have effect only in the exit plan and not in the plume beyond the cathode environment. Future experiments on this result must be done as RPA analysis in the plan of a symmetry of the cathode. However, it seems that this dissymmetry does not disturb the axis of the thrust.

Electrons properties by electrostatic probes

Electrostatics probes are one of the diagnostics currently applied to the study the properties of plasma thrusters. Two electrostatics probes are placed permanently in the PIVOINE vacuum chamber, one is a plane probe situated just above the exit plan of the thrusters (opposite side of the cathode), the second one is located in the plasma plume.
In the present paper, we are interested by the plasma area of the hot hollow cathode MIREA. The study of the behaviour of the electrons in this region is undertaken by the analysis of the probes characteristics obtained at the hollow cathode exit.

Technical description of the probes

Two series of measurements was performed with a single cylindrical probe: *serie1*: the probe was stuck on the body of the cathode (1.5cm vertical and 1.125cm horizontal from the orifice), as is it shown on the left picture of figure 15. The probe is a tungsten wire of 5mm in length and 1mm in diameter; *serie 2*: the probe is placed at the exit orifice of the hollow cathode, 2mm vertical from the orifice (on right picture of figure 15) parallel to the plane surface of the cathode. It is also a tungsten wire of 3mm in length and 1mm in diameter. The schematic view of the figure 16, shows the positioning of the probes with respect of the hollow cathode exit and the thruster channel.

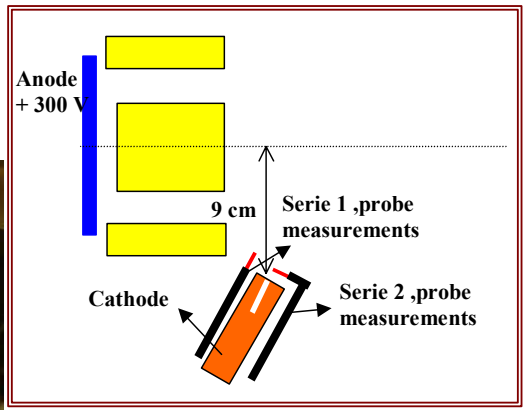

Figure 15: Pictures of the both locations of the electrostatic probes for the hot hollow cathode from MIREA
Figure 16: Schematic view of the thruster and the two probes for series 1 and 2.

The electrostatics probes are polarized with a triangular signal which frequency is 100Hz and the amplitude is ranged between –20V and +20V. The probe current is measured via a resistance of 10Ω. The acquisition of the single probes characteristics is performed with the Tektronix oscilloscope.

Results

Measurements were performed varying the thrusters operating parameters.
Figure 17 presents the probe characteristic obtained with the probe position corresponding to the serie 2 and for the following thrusters parameters: cathode mass flow rate 0.7mg/s, anode mass flow rate: 5mg/s, discharge voltage 300V. The plot shows two distinct kinks, suggesting double peaks in the electron distribution function, and this is indeed confirmed in fig 21. The method employed for the determination of the floating voltage (V_f) and the plasma voltage (V_p) from the ground voltage reference (vacuum chamber) are graphically presented in this figure. The accuracy of the plasma voltage determination is rather great because the electrons are perturbed by the presence of the magnetic field and the electronic branch is not well defined.

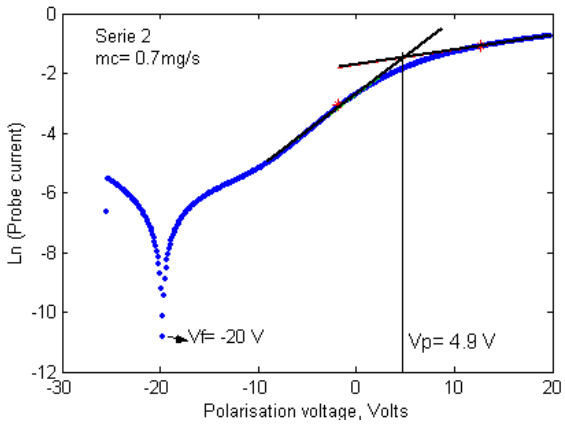

Figure17: Probe characteristic obtained for the serie 1

Probes measurements for series 1 and 2, have been performed in two times.

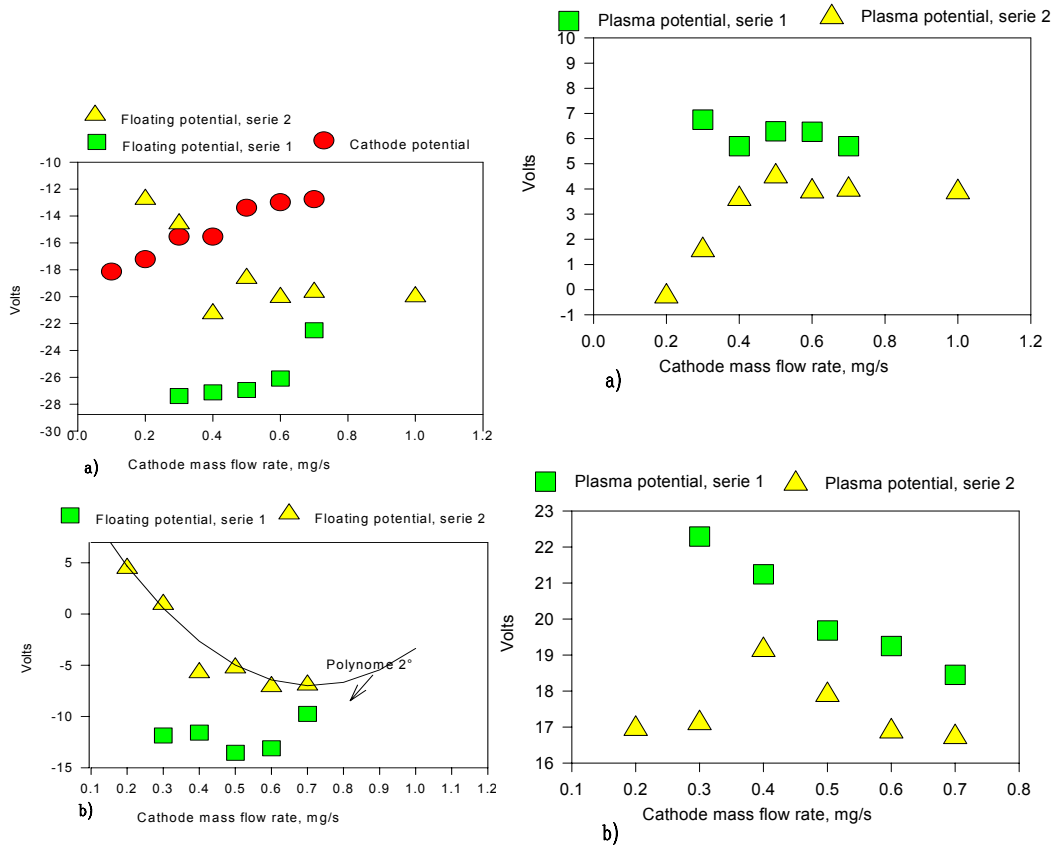

Figure 18: a) floating potential measured relative to the ground; b) floating potential calculated relative to the cathode potential. Vd= 300 V, ma=5 mg/s

Figure 19:Vd= 300 V, ma=5 mg/s a) plasma potential measured relative to the ground; b) plasma potential calculated relative to the cathode potential.

The figure 18 presents the floating potential, for the two probes positions versus the cathode mass flow rate. In figure a) the values of the floating potential and the hollow cathode potential are measured with respect to the ground. In the figure b, the floating potential is corrected with respect to the cathode potential. We note that the value of plasma potential serie 2 is lower than those of serie 1. We can explain that by the small distance between the orifice and the probe of the serie 2. The difference of potential between the probe and the cathode is connected to this distance, the electrons must observe a potential higher at the location of serie 1 than this of serie 2, if they want leave the cathode area. The plasma potential is presented in the figure 19. One can remarks that from a cathode mass flow rate of 0.4mg/s the plasma potential difference measured at the two positions near the cathode exit stays constant (about 3V). Below 0.4 mg/s the gap between both values increases.

The electron energy distribution function have been calculated from the single probes characteristics using the second numeric derivative method.

$$EEDF = \frac{4}{Se^2}\sqrt{-m_e \frac{V - V_p}{2e}} \cdot \frac{d^2 I}{dV^2}$$

Figures 20 show the EEDF curves for each cathode mass flow rate, obtained in the outlet of the cathode (serie 2) and on the side of the cathode (serie 1).

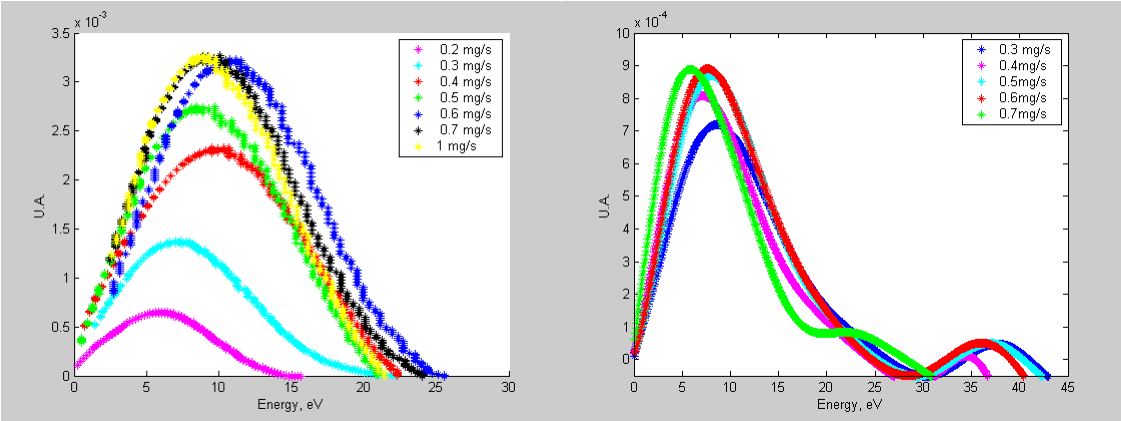

Figure 20: Electron Energy distribution functions at the outlet cathode (serie 2);Vd=300 Volts, ma=5 mg/s.
Figure21: Electron Energy distribution functions on the side of the cathode (serie 1);Vd=300 Volts, ma=5 mg/s.

The electron energy ranged between 5 and 15eV at the cathode exit, and between 5 and 10eV on the side of the cathode. For this serie 1, a second electron population seems to appear between 25 and 38eV. The second population can be explained by the difference of potential between the plasma and the cathode. If an electron doesn't undergo a collision, it gets an energy about ~e(V_f-V_c) that corresponds with the energy of this second population[1-9]. The fitting of theses electron distribution functions shows that the better form is a Druyvesteynian[12] function given by :

$$F(\varepsilon) = C\sqrt{\varepsilon}\,\exp\left[-\left(\frac{\varepsilon}{\mathrm{kTe}}\right)^2\right]$$

The reason could be the anisotropy of the cathode acceleration region and the hydrodynamic expansion leading to a rarefied regime with probably Knudsen number K_n>1. The figure 22 presents an electron distribution function obtained at the cathode exit, with a cathode mass flow rate of 1 mg/s and the fitting Druyvesteynian[9] function. As it can be observed, the agreement is very good.

For each cathode mass flow rate, it has been reported the maximum of each EEDF curve, representing the more probable energy of the electron population (figure22).
The electron energy, at the outlet of the cathode (serie 2) can be fitted by a second order polynome, where two points, 0.4 and 0.6 are out this curve fit.

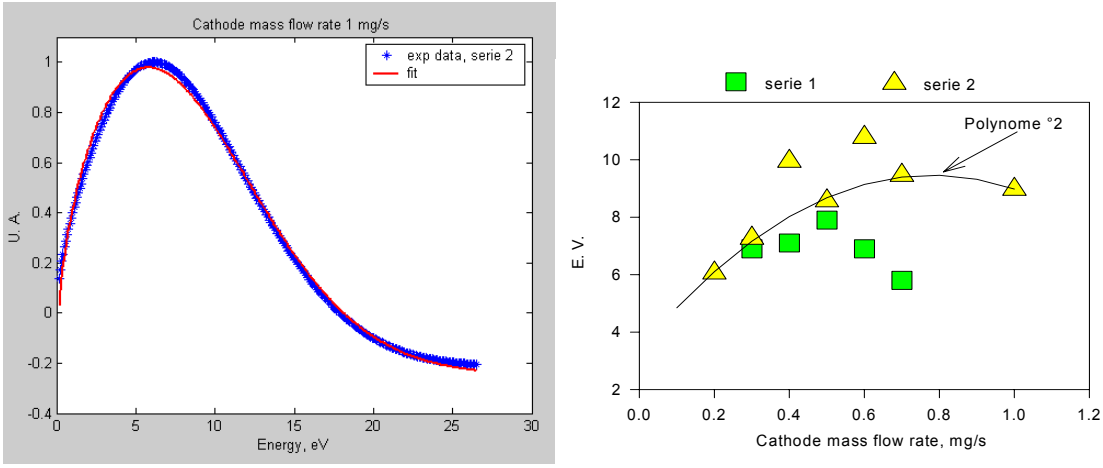

Figure 22: Fit of an experimental EEDF with a Druyvesteyn function.
Figure 22 : Electron energy measured from EEDF

It is notable to remark that the floating potential follows this inverse behaviour with the same points (almost at 0.4 mg/s) out of the fitting curve.

In the case of the serie 1, that is to say for measurements on the side of the cathode, a maximum of electron energy of 8eV is reached for a cathode mass flow rate of 0.5 mg/s, while the same point corresponds to a minimum for the floating potential (-14.8 V).
This can be explained by the meaning of the floating potential: by definition the floating potential corresponds to the potential value where the ionic current is equal to the electronic current, so to the potential value from which the electrons begin to be attracted. It means that where the value of the floating potential is very negative, electrons have to be very energetic to cross the potential wall.

It is interesting to plot the difference between the plasma potential value obtained for the two series of experiences versus the cathode mass flow rate (figure 23). Now let us compare this curve with that presented in figure 12 representing the ratio of the intensity of the ionic line 525nm between the external channel region and the near cathode region.(see page 5). We can observe that the behaviour of both curves is rigorously the same, presenting a strong asymmetry when the potential difference is maximum. It seems that the distribution of Xenon ions at the axis of the channel is linked with the plasma potential value around the cathode.

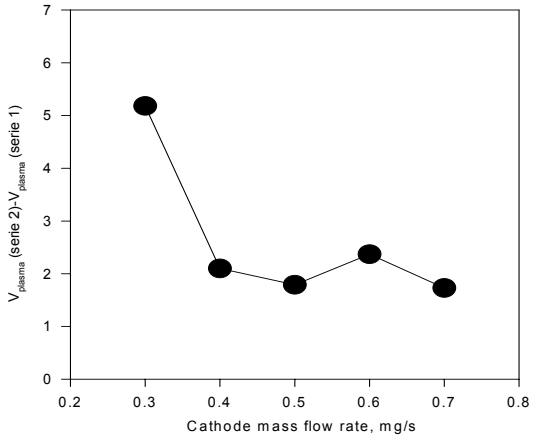

Figure 23 : Difference between the plasma potential for the two series of experiences versus the cathode mass flow rate.

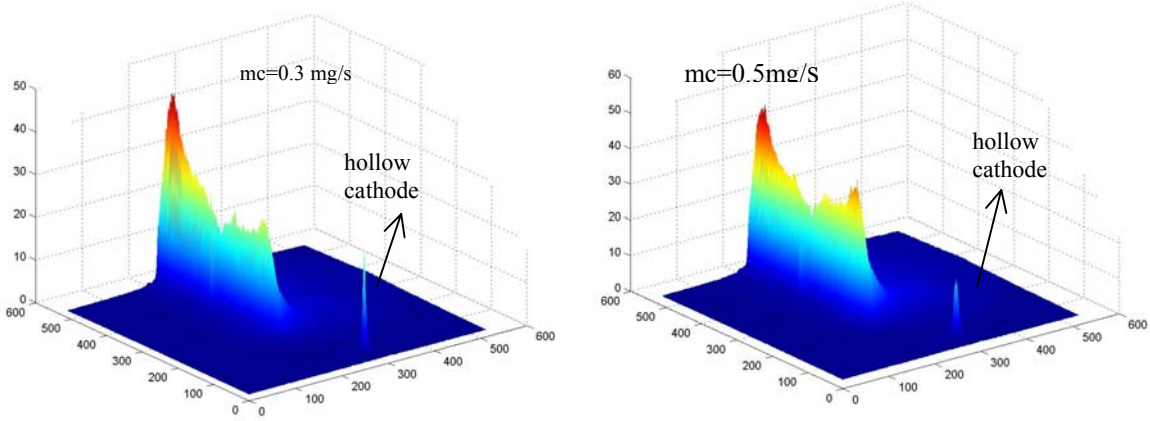

Figure 24: Ion luminous intensity distribution obtained with the CCD camera with a 525 nm filter.

The measurements by electrostatic probes show that the gas is weakly ionised at the orifice. The neutral density is evaluated by the mass flow rate[12]:

$$n_a = \frac{m_c}{M_{Xe} S_{orifice} \sqrt{\gamma R T_{orifice}}}$$

with m_c cathode mass flow rate [Kg/s], M_{Xe} is the atomic mass of xenon [kg], S the surface of orifice [m²], γ adiabatic index, R the gas constant for xenon 6.31 [J.kg^{-1}.K^{-1}], T the orifice wall temperature [K]. This formula is a upper estimation of the value of neutrals density. We obtain n_a=7,09.10^{14} cm^3. The electron current collected by the probe gives the electron density $n_e \approx 1.10^{13}$ cm^3 at the orifice if one assumes an electronic temperature about 5eV at the exit of the cathode. The ratio n_e/n_a is then

around 1.4% (value of 2% found by a worksheet model[12]). The Debye length is around 5µm that justify the interpreting of the characteristic curves. The Larmor mean free path of electrons and the Larmor radius is around 1.7mm that is comparable with the diameter of the orifice. The electron-neutral mean free path is around 0.7mm.

The zones of production of electrons

There are several zones of creation of electrons inside the cathode and also outside at the level of the orifice. These various zones of creation should give birth to various populations of electrons in energy. The electrostatic probe, the spectroscopic optical emission and CCD camera experiments gave us local information about these populations of electrons. The easier zone to observe, is the most downstream area because it can be revealing by the erosion of the orifice. This zones of creation depends strongly on the functioning cathode parameters like the mass flow rate but also the voltage discharge of the thruster.

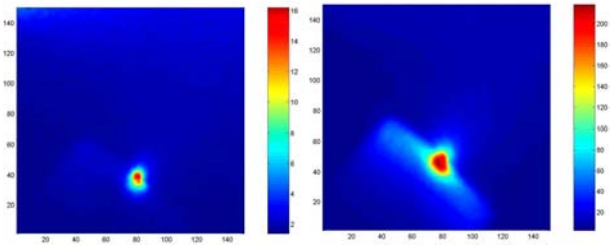

Figure 25:Image of MIREA cathode spot, m_c=0.4mg/s, m_a=5mg/s, V_d=300V 1) filter 525nm ions 2) 825nm neutrals

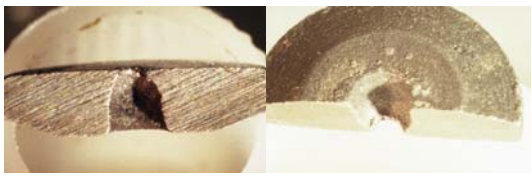

Figure 26: Images given by the KhAI, cutting of the orifice of the cathode. The eroded part faces outside, i.e. towards the spot of light

The figure 25, shows two CCD images of the exit plume cathode, one for ions and the second for neutral. In both case the great intensity emission is just at the exit of the orifice and even a little bit inside it. Comparing both pictures, it is clear that the neutrals are predominant in the cathode discharge. The measure of the ionisation ratio got by electrostatic probe has a value just superior to 1%. Between the two species of ions, line at 529nm (metastable) seems to be more intense than this at 460.2nm.

On the images[8] (figure 26) of erosion, we can see that the eroded part faces the outside where the bombardment of the ions is the more intense. Indeed, the ions created in the luminous spot of the cathode are attracted by the strongly negative potential of the cathode and strike the surface of the orifice. The erosion occurs also inside the length of the orifice and it modifies even the shape of this constriction. It exists some electrons creation area in the cathode and just outside the orifice. Now, we present (figure 27) the most downstream zone just at and inside the orifice. With the CCD camera we can explore the ions and excited neutrals. In the orifice area, there's a constriction that creates a huge density of particles and a large number of collisions with the orifice's surface.

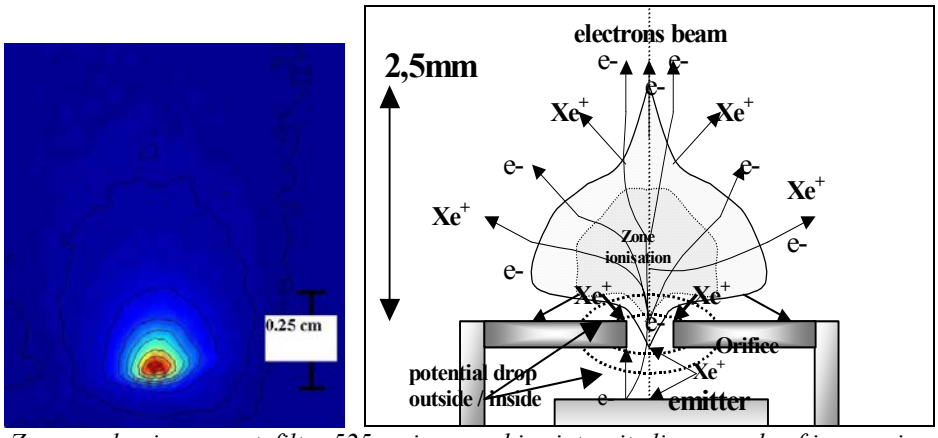

Figure 27: Zoom on luminous spot, filter 525nm ions, and iso intensity lines, scale of image gives size about 2.5mm of height.

Figure 28: *Small draw (without respect of scale) of luminous spot at the exit of the orifice.*

The cathode discharge is at a negative potential (cathode potential) what tends to repel the electrons and attract ions. Before going through the orifice, some ions move by ambipolar[17] diffusion or are pulled by the flow of neutral gas towards the orifice area. In this constriction zone a double layer[14] accelerates electrons and repels ions. Therefore, it is difficult to have electro-neutrality, besides a bit of ions, which manage to reach this zone (and also neutrals) do a lot of collisions with the wall of the orifice ($\lambda_{collision} << L$ or D , with L length and D diameter, orifice dimensions).

These collisions favour the recombination of ions with the surface. A consequence is a lack of positive charges and excess of electrons. At the downstream of the orifice a second double layer appears to expulse and accelerate electrons outside. Electrons get enough energy to ionise the neutrals, these created ions are attracted by this double layer[14] into the orifice with a high velocity to balance the electric charges. Ions erode the surface of the orifice but only on the outside face (figure 28).

The results of the EEDF, by the electrostatic probe in the orifice area, show that electrons seem to be thermalized by the collisions because of the Druyvesteyn shape of the curve and by the presence of electric potential structures. In fact at the exit of the orifice, it is impossible to go back up to the roots of electrons. They are created by thermo-emission[15], ionisation[15] in the tube and by electron-neutral collision in the plasma bulk in the luminous spot. After the crossing through the orifice, density of particles implies a very small intercollisional length. All particles are thermalized and homogenized in the luminous spot.

Zone of electronic transport by CCD camera

It is possible to define a area located from the orifice of the cathode to the contact between the thrusters jet and cathode plume. We call this area : ”zone of electronic transport” because it is by this zone that electrons reach the main discharge of the SPT. The physical process which allows the electrons to cross the lines of magnetic field and the potential map is not well understood, as well as the mechanism which allows to separate the electronic current on one hand to supply the discharge and on the other hand to neutralize the space charge. This experiment gave us information about size and the shape of this electronic transport zone. By means of a CCD camera associated with the filter 825nm, we can observe excited neutrals. Therefore, by analogy, we can say that we follows the electrons which excite the neutral atoms. The low pressure in the cathode area, the short lifetime of the spectroscopic line and the EEDF of electrons show that electrons have enough energy to excite neutral atoms from the fundamental level to the excited level and the transition appears quickly. Like this, we do not observe an atom excited from the orifice to the end of electronic transport area but we observe, along all the path, the xenon atoms which are excited continuously by the electrons.

Line nm	Atoms	E_2	E_1	E eV
823,2	Xe I	2p6	1s5	9.82
828,0	Xe I	2p5	fond	9.93

Table 2 main excited neutral lines and their energies

Beyond this area, the luminous intensity of the thruster plume hides completely the intensity of the cathode zone. Moreover, we have to carefully centre the picture because the intensity of the luminous spot of the cathode and the cathode body are sometimes too much intense. In this case it becomes very difficult to make appear the electronic transport zone.

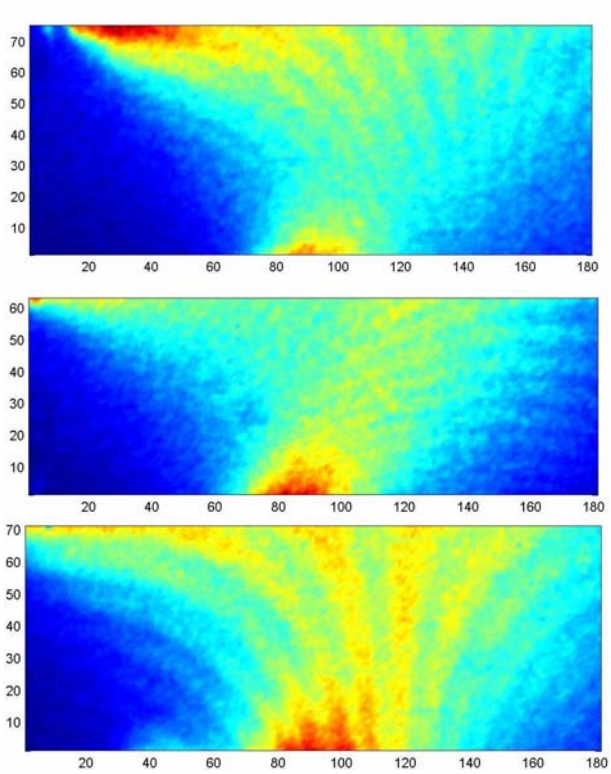

Figure 29: Zone of electronic transport between the cathode and the thruster plume filter 825nm, high :cathode KhAI, scale 1cm->37.5 pixels center cathode LABEN scale 1cm->38.3pixels, down cathode MIREA scale 1cm->28 pixels

We also try to explore the area to use the other filters 525 and 450nm. But the ratio signal noise is worst with this both filters than with the 825nm because of the intensity of ionic emission in the plume. We can compare the three pictures of electronic transport in the cathode area (figure 29). We note that area of the cathodes KhAI and LABEN seem to be almost identical while the cathode MIREA presents a shape different. The last picture shows a large width band of transport about 70 pixels whereas the others width are about 40 or 50 pixels. It seems to be more vertical than these of the other cathodes at the orifice exit. The orifice has a large size and thermal shield are not optimised. An important part of heating power is lost by thermal radiation outside the cathode body. This cathode is far from being optimised. A rather thin beam appears toward the height on both first pictures. From the orifice to the first thirty pixels and beyond this height, the beam widens more and more and finally reaches the plume of the thruster.
Therefore, we can define two parts in the electronic transport area of the cathode. The first one seems to be a electron beam (thin part on the picture) and second one where the beam widens more and more. This is in the second part that electrons could operates the separation between the discharge and the neutralisation of the plume. An experiment with a fast switch system[2-10] set up (from the laboratory GREMI) on the anode electric line allows us to create a series of cuts in the discharge. These 1µs to 15µs cuts have a frequency of 100kHz. The characteristics of the discharge are then frozen during the time of the cut. Therefore, there's no more electric field or electronic transport towards the anode, we keep the electro-neutrality in the channel but the cathode must carry on to neutralize the plume. Therefore, we can measure the electronic current which involves to neutralize and we know the value of the discharge current at the anode.

$$I_{d\,total} = I_{d\,e} + I_{d\,N} = 4.23A$$

with I_{de} electronic current in the direction of the channel, I_{dN} electronic current of neutralisation into the plume

The value of neutralisation current is about 3.34A, then the electronic current which supply the discharge is about 0.89A. The measure has been done with the KhAI cathode because this cathode is connected to electric circuit by only one wire whereas the others are connected by several wires by

which we can have losses of current (heater or electrode wire). The measurement is difficult and not already optimal because of oscillation and electromagnetic pulse due to the impulse of the cut. A new experiment is foreseen to improve the accuracy of the value. A numerical model[18] (2D channel and plume) done by the CPAT (Toulouse laboratory) gives 0.9A for the electron current which reaches the channel. Then, there's a good agreement between the model and the experimental work on this part.

Study of luminous spot at the orifice of the cathode by optical spectroscopic emission

The analysis of the luminous intensity emission of the spot light of the cathodes, have been studied with an optical spectroscopy set up. Optical measurements have been performed with a spectrometer (AVANTES AVS-USB2000) and the spectral range explored extends between 400 nm to 850 nm. A lens has been used to focus and collect only, on the slit of the optic fibber, the light emitted by the cathode spot without crossing the light emitted by the plume of the thruster.
We recorded a large number of lines and we selected 6 ones, resumed in table 3, which are the most intense.

specie	λ nm	g_i-g_k	τ μs	*Emitting level*	*Excited from*	$\Delta(E_k-E_i)$
Xe I	467,1	5–7	ng	3p8	1s5	2.69 eV
Xe I	823,1	5-5	2.7	2p6	1s5	9.81 eV
Xe I	828,0	3-1	1.2	2p5	Xe I fund	9.93 eV
Xe II	484,4	6-8	1.9	$6p^4D^0_{7/2}$	$5d^4D_{7/2}$	2.27 eV
Xe II	529,2	6-6	2	$6p^4P_{5/2}$	$5d^4D_{7/2}$	2.06 eV
Xe II	541,9	4-6	ng	ng	ng	2.28 eV

Table 3: selected lines

The goal of this optical study is to analyse the composition of the Xenon plasma in the spot-light of cathodes with the variation of the thrusters functioning parameters (anode and cathode mass flow rate, discharge voltage). This optical study was realised with MIREA and LABEN cathodes.

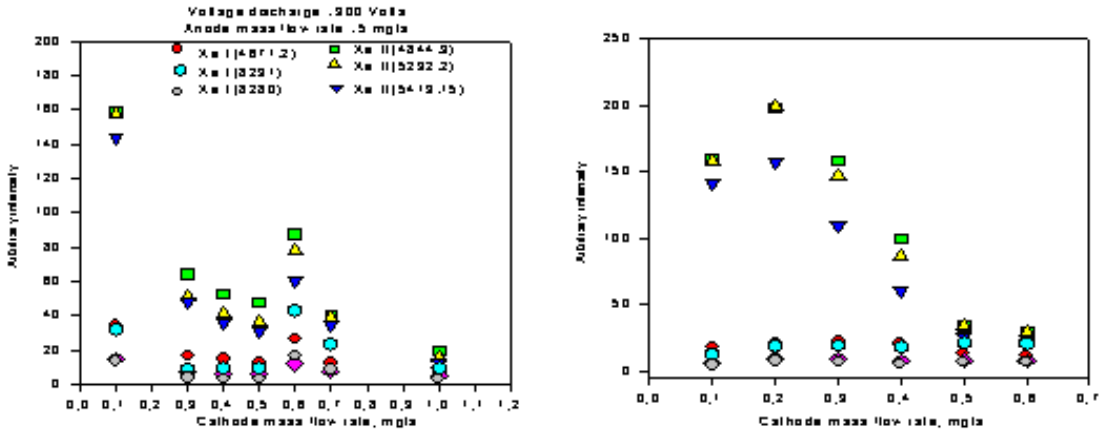

Figure 30: Evolution of the line intensity as a function of the cathode mass flow rate a) Mirea cathode, b) Laben cathode

The evolution of the emission with the cathode mass flow rate, for both cathodes, presents a decreases from a value of 0.2 mg/s. Also the emission from ions is greater than the emission from neutral, which variation is constant with the mass flow rate. This results correlate with those obtained with the CCD camera. Moreover, the comparison between the intensity of ion emission recorded with the CCD camera, presented in figure 24, and the emission recorded with the optical spectroscopy (figure 30) shows the good agreement of this results.
It is interesting to remark that the evolution of the ionic lines with the cathode mass flow rate (figure 30 a) follows the same variation than the difference of the plasma potential obtained with the

electrostatics probes for the MIREA cathode, (figure 23). It could be due to the acceleration more important for low mass flow rate, giving more energy to electrons which are more able to ionise the Xenon .
As the neutral emission is constant with the cathode mass flow rate, the ratio between the ion intensity and the neutral intensity decreases to 1 (at 1mg/s) with the cathode mass flow rate, except the discontinuity at 0.6 mg/s. Linking this result with those concerning the dissymmetry of the ion emission (figure 12), one can find that at low mass flow rate, when the intensity of ions at the cathode exit is maximum the dissymmetry also, that is to say that at the exit thrusters the ions are more concentrated on the opposite side of the cathode. When the ion emission at the cathode decreases, we find this ions at the near side of the cathode of the thrusters exit. The figure 31 illustrates this results. So at least for the MIREA cathode, the cathode mass flow rate has an influence on the distribution of the plasma potential and on the distribution of Xenon ion, the neutrals don't seem to be affected.

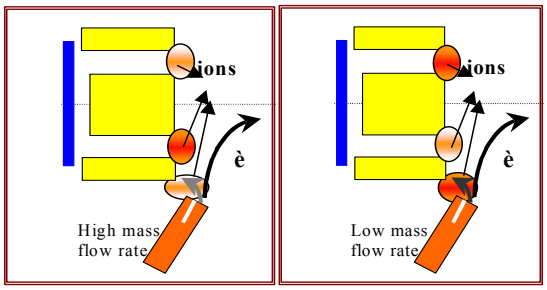

Figure 31: Influence of the cathode mass flow rate on the distribution of ions

It is interesting to note that the discontinuity for a mass flow rate of 0.6 mg/s, appears for all the measurements, which were recorded at different times, and the results agree between them.

Mode Spot et mode Plume

The existence of two modes of functioning SPOT & PLUME has often be seen in diode regime for the cathode. In our experiments with a Hall thruster we didn't see this transition with the cathode MIREA with a large orifice. The transition between the two modes has been observed with the cathode KhAI (figure 34). The reason is certainly the dimensions of the orifice, which are smaller than the MIREA and LABEN cathode orifices. The small dimensions of the orifice favour the phenomenon of effusion of the gas flow and increase the constriction of the cathode discharge. It seems that these two modes are connected with the cathode mass flow rate and with the voltage discharge applied to the discharge.

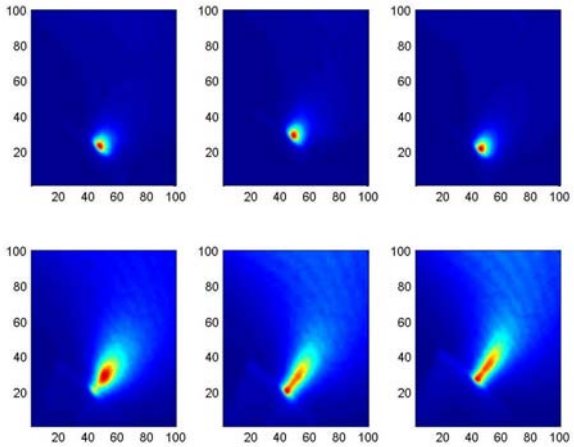

Figure 34: Images of the exit of the orifice, transition mode SPOT/PLUME with the cathode KhAI filter 825nm (neutrals), cathode mass flow rate 0.2, 0.3, 0.4, 0.5, 0.6, 0.7 mg/s with m_a=5mg/s and V_d=300V

A physical explanation of these modes is often quoted as a sonic shock resulting from the pressure inside the cathode which increases as the cathode mass flow rate. The potential around the cathode

certainly plays role since when varying the applied voltage at constant flow we can observe the mentioned transition. Pressure inside the cathode increase with the cathode mass flow rate and reaches the critic value. Then the flow becomes supersonic, besides the density of neutral gas inside the tube is largely superior than the ions one. The neutral gas controls the flow. When the flow rate increases the cathode potential decreases. Therefore electrical force or electrical structure as the double layer can not involve as at low flow rate on electrons and ions.
The properties of the spot and plume modes seem to be only depending of the cathode operating conditions. In order to precise this point, a comparison for the same conditions of pressure and mass flow with the three cathodes in a diode regime will permit to acquire a better understanding of these modes. Another advantage of these tests can be find of a comparison of the behaviour of the thruster in order to justify the validity of the tests in diode regime. More, it is known that the spot mode is more advantageous for the global performances of the thusters. This point has to be analyzed.

Conclusion

A study of various hollow cathodes suitable for stationary plasma thrusters have been carried out.
Optical spectroscopy and probe measurements have been carried out for the analysis of the plasma near the orifice. The electron temperature and the plasma potential have been measured at two locations near the cathode exit. The two emitted currents (for the plume neutralization and for the ionization) have been measured and the values are in good agreement with a 2D numerical code. We have shown : that an increase in the oscillations of the discharge current is a function of the cathode mass flow rate; there is an asymmetry of the plume due to the cathode; Druyvestinyan function appears to be the most appropriate electron energy distribution function at the exit of the orifice and that the neutral species are the majority species near the orifice.
However some of the observed effects, in particular the plume asymmetry and its coupling between the cathode discharge are not fully understood and further research programme is planned to elucidate these and other aspects of the cathode discharge plasma. In addition to electrostatic probes and CCD camera, it is planned to use a ‘fast switch’ system to determine the electron flow distribution between the plasma discharge and the neutralization zones. A numerical model and time resolved CCD pictures will also be attempted to understand in detail the electron transport within the cathode channel region. An exploration from the orifice of the cathode to the exit plan of the channel by an electrostatic probe on a moving system is foreseen. In order to measure plasma parameters and also to study signals from the oscillations in HF.

Acknowledge

This work has been performed in the frame of the Groupement de Recherche CNRS/CNES/ SNECMA/ONERA n°2232 "Propulsion à Plasma pour Systèmes Spatiaux". We want to thank specially Andrey Loyan from the KhAI in Ukraine for his technical and theorical help during the experiments and the comments on the article. A special thanks for Sisouk Sayamath for his technical help during the experimental work.

References

1. - Etude de la physique interne d’un propulseur à plasma stationnaire par spectroscopie optique d’émission. Mise au point d’un analyseur électrostatique de type MASON. *Thesis Philippe Leray, laboratoire LPGP, university PARIS XI Orsay 1999, France*
2. - Etude expérimentale des propulseurs de type Hall, processus collisionnels, comportement dynamique, micro instabilités et phénomène de transport *Thesis Mathieu Prioul, GREMI, university Orleans, 2002, France*
3. - Etude de propulseur plasmique à effet Hall pour système spatiaux. Performances, propriétés des décharges et modélisation hydrodynamique. *Thesis Nicolas Gascon, Aérothermique, university of Provence, 2000, France*

4. - Analyse par spectroscopie optique d'émission du plasma des propulseurs à effet Hall application à l'érosion des céramiques. *Thesis Stéphanie Roche, LPGP, university PARIS XI Orsay, 2000, France*
5. - Etude expérimentale des phénomènes de décharge et propagation d'ondes dans les propulseurs ioniques à dérive d'électrons en cycle fermé. *Thesis Gilles Guerrini, laboratoire PMI, university of Provence, 1997, France*
6. - Hall thrusters cathode coupling *AIAA paper 99 DL, Tilley, KH de Grys, RM Myers Primex aerospace Co Redmond, WA*
7. - private communication V. Kim (RIAME Moscow),
8. - private communication A. Loyan (KhAI Kharkov Ukraine),
9. - Electron density and energy distribution function in the plume of a Hall type thruster *Review of scientific instrument vol 73 n° 2 Feb 2002 M. Baccal, AA Pereslavtsev & al*
10. - Insights on physics of hall thrusters throught fast current interruptions and discharge transients, *IEPC paper 2001- 059 M. Prioul, A, Bouchoule, & al*
11. - Theory of hollow cathode operation in spot and plume modes. *Mandell, M.J and Katz I, AIAA paper 94-3131 30th AIAA/ASME/SAE/ASEE Joint propulsion conference, Indianapolis IN, June 1994*
12. - Evaluation of low current orificed hollow cathodes *M. T. Domonkos, University of Michigan 1999 USA*
13. - Transport property and mass spectral measurements in the plume of a Hall effect space propulsion system *King, thesis university Michigan 1998*
14. - Structure of the double sheath in a hot cathode plasma *F.W Crawford A.B Cannara 1965 Journal of Applied Physics.*
15. - Spectroscopic measurements of the plasma within a hollow cathode Monterde, Dangor, Haines, K. Malik, Imperial College London AIAA 95
16. - Correlation between Hollow Cathode operating conditions and Hall Thruster (SPT100-ML) performances L. Albarede,.V. Lago, P. Lasgorceix, M. Dudeck, AIAA- 2002- 4101 Indianapolis
17. - Theorie de la décharge d'arc à cathode creuse application à l'Argon, Thesis, Almeida Ferreira, LPGP université Orsay 1976
18. - Modelisation 2D hybride d'un propulseur à effet Hall pour satellites, Thesis, Jerome Bareilles, CPAT, université Paul Sabatier de Toulouse, 2002, France
19. - Private report N 682, 3 mars 2000, Brugova.